separation accompanied by crystallization of PC phase. The casting from MC solutions gives modulated structure, but no crystallization is involved. Time-resolved light scattering studies on PC/PMMA/THF system is characterized by the early stage of spinodal decomposition; however, the linearized Cahn's theory is found inadequate. In the case of PC/PMMA/MC system, the power-law scheme prevails characterizing the late stage of spinodal decomposition.

Acknowledgment. A partial support from Edison Polymer Innovation Corp. (EPIC) is gratefully acknowledged.

Registry No. PC (copolymer), 25037-45-0; PC (SRU), 24936-68-3; PMMA, 9011-14-7.

References and Notes

(1) Olabisi, O.; Robeson, L. M.; Shaw, M. T. *Polymer Polymer Miscibility*; Academic: New York, 1979.
(2) MacMaster, L. P. *Adv. Chem. Ser.* **1975**, *No. 142*, 43.
(3) Nishi, T.; Wang, T. T.; Kwei, T. K. *Macromolecules* **1975**, *8*, 227.
(4) Gilmer, J., Goldstein, N., and Stein, R. S., *J. Polym. Sci., Polym. Phys. Ed.* **1982**, *20*, 2219.
(5) Nojima, S.; Nose, T. *Polym. J.* **1982**, *14*, 269; **1982**, *14*, 907.
(6) Hashimoto, T.; Kumaki, J.; Kawai, H. *Macromolecules* **1983**, *16*, 641.
(7) Snyder, H. L.; Meakin, P.; Reich, S. *Macromolecules* **1983**, *16*, 757.
(8) Hill, R. G.; Tomlins, P. E.; Higgins, J. S. *Macromolecules* **1985**, *18*, 2555.
(9) Voigt-Martin, I. G.; Leister, K. H.; Rosenau, R.; Koningsveld, R. *J. Polym. Sci., Polym. Phys. Ed.* **1986**, *24*, 723.
(10) Varnell, D. F.; Runt, J. P.; Coleman, M. M. *Macromolecules* **1981**, *14*, 1350.
(11) Inoue, T.; Ougizawa, T.; Yasuda, O.; Miyasaka, K. *Macromolecules* **1985**, *18*, 57.
(12) Zeeman, K.; Patterson, D. *Macromolecules* **1972**, *5*, 513.
(13) Hashimoto, T.; Sasaki, K.; Kawai, H. *Macromolecules* **1984**, *17*, 2812. Sasaki, K.; Hashimoto, T. *Macromolecules* **1984**, *17*, 2818.
(14) Note that H_v cross polars are slightly offset in order to accentuate the inner scattering halo.
(15) Stein, R. S.; Wilson, P. R. *J. Appl. Phys.* **1962**, *33*, 1914.
(16) Kyu, T.; Saldanha, J. M., *Macromolecules*, submitted for publication.
(17) Kyu, T.; Saldanha, J. M. *J. Polym. Sci., Polym. Lett. Ed.*, submitted for publication.
(18) Cahn, J. W. *J. Chem. Phys.* **1965**, *42*, 93.
(19) Stein, R. S.; Rhodes, M. B. *J. Appl. Phys.* **1960**, *31*, 1873.
(20) Binder, K.; Stauffer, D. *Phys. Rev. Lett.* **1974**, *33*, 1006.
(21) Siggia, E. D. *Phys. Rev. A* **1979**, *20*, 595.

Configurational Properties of a Terminally Attached Chain at the Boundary of a Molecularly Coarse Solvent

Clive A. Croxton

Department of Mathematics, University of Newcastle, NSW 2308, Australia.
Received January 20, 1987

ABSTRACT: The effect of solvent composition (solvent particle diameter and packing fraction) upon the configurational properties of hard-sphere chains terminally attached to a rigid boundary is investigated on the basis of the iterative convolution (IC) approximation. It is found that the segment density profile normal to the boundary develops pronounced oscillations of period equal to the solvent diameter and amplitude depending upon solvent packing fraction. The contact amplitude at the boundary develops dramatically as solvent diameter decreases, with important implications for the development of loop and train configurations. We also find that the mean thickness of the adsorbed layers, the mean square end-to-end length, and the mean square radius of gyration all decrease with the introduction of solvent.

Introduction

Considerable theoretical attention has been focused on the description of the configurational properties of terminally attached chains in the vicinity of a rigid plane boundary since the problem has implications for a wide variety of phenomena ranging from applications in chemical engineering to aspects of cell biology. These studies may be broadly resolved into lattice-based and continuum analyses in which a variety of exact enumeration, Monte Carlo, and other analytical and numerical techniques have been applied. While the self-avoiding feature is accounted for to a varying and approximate degree in these studies, the role of the solvent in determining the configurational properties of the chain has received little attention. Certainly, chains embedded in a regular lattice to a certain degree reflect the molecular coarseness of the solvent, but only in as far as the lattice provides an adequate representation of the surrounding fluid, which by any other standard it does not. Nevertheless, in an earlier study by Bellermans and De Vos,[1] the ratio of the mean-square lengths $\langle R_{1N}^2\rangle_\eta/\langle R_{1N}^2\rangle_{\eta=0}$ for athermal chains embedded in a simple cubic lattice was investigated as a function of chain packing fraction η. Each site may be occupied either by one element of a chain molecule or by a solvent molecule. At low to intermediate concentrations the ratio decreases almost linearly with η:

$$\langle R_{1N}^2\rangle_\eta/\langle R_{1N}^2\rangle_{\eta=0} \sim 1 - 0.04(N-1)^{0.7}\eta + \ldots$$

A similar, but nonlinear, dependence was found on the basis of a continuum convolution analysis at intermediate to high packing fractions,[2] becoming quadratic ($N < 11$) and then cubic ($12 < N < 20$) with increasing chain length.

In a previous publication[2] we reported the configurational properties of an isolated athermal self-avoiding chain in a solvent of its own segments on the basis of a convolution integral approximation. The results were extended to include the equation of state at intermediate to high polymer packing fractions, and recent Monte Carlo simulations appear to be in excellent agreement with those predictions.[3] Since then, the technique has been superseded by an iterative convolution approach (IC), which for short to intermediate length sequences ($N < 25$ segments) appears to yield configurational properties in good quantitative agreement with Monte Carlo simulation studies.[7]

It was found that the spatial probability distributions $Z(r_{ij}|N)$ of segments i,j within the isolated N-mer were

0024-9297/87/2220-2847$01.50/0

profoundly modified with increasing solvent packing fraction, η, and we anticipate similar effects for terminally attached sequences. The presence of a surrounding molecularly coarse solvent was accounted for in terms of an effective potential of mean force $\Psi(r_{ij}|\eta)$ developed between pairs i,j of segments immersed in the solvent, while the effect of the boundary is introduced as in the previous studies[5-7] by observing the properties of the sequence 1, ..., N as the diameter of the terminal segment $\sigma_0 \rightarrow \infty$. In practice, approximations additional to those inherent in the iterative convolution technique are introduced, and these will be discussed in detail below. However, at this stage it is sufficient to say that $\Psi(r_{ij}|\eta)$ is determined in the Percus–Yevick (PY) approximation on the basis of the Ornstein–Zernike (OZ) integral equation, while previous experience suggests[5] that configurational properties of the sequence at a plane boundary are rapidly attained with increasing σ_0, and in fact $\sigma_0 = 64\sigma_i$ (σ_i = chain segment diameter) is assumed throughout. We also note that with decreasing packing fraction $L t \eta \rightarrow 0 \Psi(r_{ij}|\eta) \rightarrow \Phi(r_{ij})$, the direct interaction potential.

Configurational properties of the chain are determined on the basis of a knowledge of the complete set of intramolecular spatial probability distributions $Z(r_{ij}|N)$ developed between a pair of segments i,j wihin the linear, heterogeneous, sequentially connected system of central pairwise interactions which define the polymer sequence, although for present purposes we restrict ourselves to a linear homogeneous sequence of hard-sphere segments. The model is of considerable versatility and has already been used to describe isolated[4] and terminally attached sequences, ring polymers, flocculation, and stabilization of emulsions, and the development of loops, trains, and tails at a rigid boundary (see ref 6). While an exact account of the excluded-volume problem is unlikely to be achieved, the IC approximation does appear to yield results in very good quantitative agreement with Monte Carlo studies for hard-sphere systems which forms the basis of our confidence in the technique.

The OZ–PY Potential of Mean Force

We consider a uniform three-component fluid system of species α, β, and γ, present at packing fractions η_α, η_β, and η_γ, respectively. The radial distribution function $g^{\mu\nu}(r_{ij})$ expressed as a function of the separation r_{ij} between species μ and ν ($\mu, \nu = \alpha, \beta, \gamma$) is related to the potential of mean force as

$$g^{\mu\nu}(r_{ij}) = \exp(-\Psi_{\mu\nu}(r_{ij})/kT) \tag{1}$$

where kT is the usual Boltzmann factor. Clearly, a complete structural specification will involve the six distinct distributions $g^{\mu\nu}(ij)$ ($=g^{\nu\mu}(ji)$) over the dummy indices μ, $\nu = \alpha, \beta, \gamma$ together with their associated potentials of mean force $\Psi_{\mu\nu}(ij)$, where we set $r_{ij} \equiv ij$ without ambiguity throughout. These latter functions express the effective interaction potential between two particles of species μ,ν immersed in the ternary fluid system at total packing fraction $\eta_\alpha + \eta_\beta + \eta_\gamma$.

A generalization of the Ornstein–Zernike equation to a multicomponent system relates the direct $c(r)$ and total correlation $h(r)$ operating between a pair of particles through the usual convolution integral expression. Thus, for a uniform three-component system

$$h_{\mu\nu}(12) = c_{\mu\nu}(12) + \sum_{n=1}^{3} \rho_n \int h_{\nu n}(23) c_{\mu n}(13)\, \mathrm{d}3 \tag{2}$$

where the indices $\mu = \alpha, \beta, \gamma$, $\nu = \alpha, \beta, \gamma$, and η_n are run over the component species and $\rho_n = 6\eta_n/\pi\sigma_n^3$ represents the number density of species n and $h_{\mu\nu}(12) = g^{\mu\nu}(12) - 1$. Equivalence of label inversion ($\mu\nu \equiv \nu\mu$) is assumed throughout, ensuring number balance among the components. Equation 2 is evaluated in the PY approximation by fast Fourier transform techniques.

The potential of mean force developed between two particles of species μ, ν at separation r_{ij} then follows directly as

$$\Psi_{\mu\nu}(r_{ij}) = \Phi_{\mu\nu}(r_{ij}) - kT \ln (1 + h_{\mu\nu}(r_{ij}) - c_{\mu\nu}(r_{ij})) \tag{3}$$

which clearly identifies the essentially entropic modification to the "true" interaction $\Phi_{\mu\nu}$ due to the presence of the surrounding ternary solvent.

The three hard-sphere-component species α, β, and γ correspond in the present case to the "boundary", segment, and solvent particles, respectively. It is clear for an isolated terminally attached sequence in a dense solvent that ρ_α, $\rho_\beta \rightarrow 0$, while ρ_γ remains finite. It should be realized that although no $\alpha\alpha$ or $\beta\beta$ functions arise in the iteration, the segment/boundary ($g^{\alpha\beta}(r_{ij})$) and segment/segment ($g^{\beta\beta}(r_{ij})$) distributions and potentials of mean force *are* determined. It is these ρ_γ-dependent effective interactions operating between segments and the boundary and within the macromolecule itself which represent the effect of a molecularly coarse environment. It is appropriate to mention that the structure of the solvent itself is modified by the presence of the boundary through the $\alpha\gamma$ functions involved in the iteration and as such represents an important aspect of the determination of the configurational properties of the macromolecule. Incidentally, just such a screened potential description of the equation of state of dense entanglements of polymers at intermediate to high packing fractions[2] yields results in very close numerical agreement with recent Monte Carlo determinations,[3] and to that extent confidence in this approach is justified.

In the case of a hard sphere system such as that considered here, the PY approximation is known to be particularly good; moreover the $\exp(-\Phi_{\alpha\beta}(ij)/kT)$ are simply truncation functions which substantially expedite the numerical analysis. An additional advantage concerns the assumption of pairwise additivity of the potential functions, which is exact in the case of hard spheres, and to that extent eliminates a further aspect of approximation from the problem.

These OZ–PY estimates of the pair distributions and their associated potentials of mean force are, of course, spherically symmetric and determined at vanishing local segment density. This approach takes no account of sequential connectivity which excludes solvent from regions occupied by the chain itself and local modification of solvent structure. Similar observations are appropriate in the determination of the effective segment/boundary interaction. While the complex multibody correlation problem appropriate to flexible molecules has been confronted by other workers,[11] at least for short sequences, its introduction in the present approximate description is unwarranted, particularly for the substantially longer sequences under consideration here. We observe that for "good" solvents in which the sequence is maximally exposed to its surroundings the assumption of vanishing local segment density is unlikely to seriously modify the conclusions drawn on the basis of a full multibody description. Moreover, although the decoupling of the system is made for the purposes of calculation of the potentials of mean force, we emphasize that in the convolution integral description of the chain per se sequential connectivity of the system is taken fully into account.

Finally, we should also point out that the assumption of pairwise decomposability of the potentials of mean force,

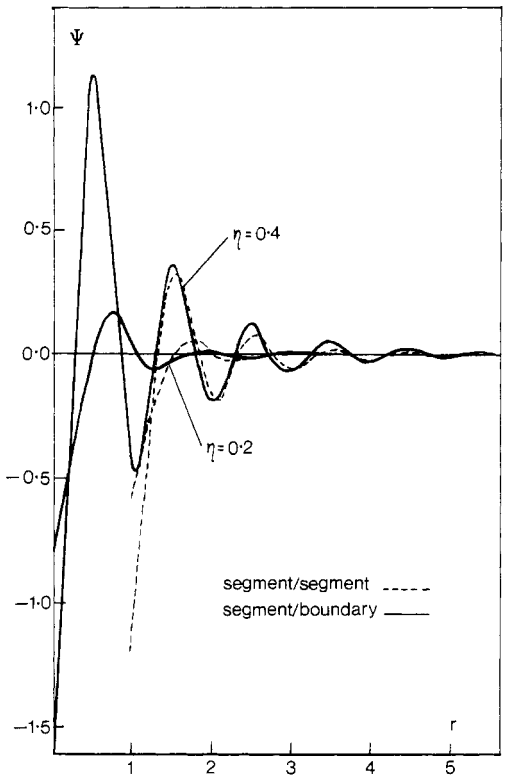

Figure 1. PY hard-sphere potentials of mean force Ψ segment/boundary and Ψ segment/segment determined for a solvent diameter $\sigma_s = 1$ at solvent packing fraction $\eta = 0.2, 0.4$.

although frequently made, is known to be somewhat less accurate than the corresponding assumption of pairwise additivity of the "raw" potential functions and, while not likely to modify the conclusions drawn here, is nevertheless a basic feature of the present treatment.

As expected from eq 3 $\Psi_{\mu\nu} \rightarrow \Phi_{\mu\nu}$ as the solvent number density $\rho \rightarrow 0$ (we drop the solvent subscript γ from now on without ambiguity) and this is clearly apparent from the potentials of mean force shown in Figure 1. The oscillations reflect the structure of the solvent in the vicinity of the chain and the boundary and would be absent in any continuum or lattice-based representation of the solvent: accordingly, the configurational properties of the chain itself are expected to reflect the structural inhomogeneity of the boundary/solvent interfacial zone.

The Iterative Convolution Approximation

The iterative convolution (IC) approximation has been described in detail elsewhere[4] and it is not appropriate to review that description here. Nevertheless, a brief outline would be useful and enables us to draw attention to those aspects of particular relevance here.

Basically, the IC approximation provides an integral equation relationship between the segmental interaction potential and the spatial probability distribution $Z(r_{ij}|N)$ of segments i,j within the N-mer. A knowledge of the complete set of internal distributions $Z(ij|N) N \geq i > j \geq 1$ within the sequence yields all the principal geometric moments of the molecule, such as mean square length, radius of gyration, etc.

Since the segments of the chain are not equivalent, each bead is, in effect, a different component in a "mixture". This may be indicated explicitly in the basic integral equation as follows:[4]

$$Z_{ij}(12|N) = aH_{ij}(12)\Pi' \int Z_{ik}(13|N)Z_{kj}(32|N)\ \mathrm{d}3 \quad (4)$$

in an obvious notation, where a is a normalization constant, $H(ij) = \exp(-\Phi(r_{ij})/kT)$ explicitly introduces self-interaction within the system, and Π' represents the geometric mean of the set of convolution integrals, excluding $k = i,j$. The above ansatz expresses the spatial correlation between segments i,j as propogating through the direct interaction $H(ij)$ and the mean of all possible indirect routes via the sequence: it should be emphasized that these indirect routes may involve up to $N - 2$ mediating segments and not merely a third field particle k as eq 4 might suggest.

The above integral equation provides what is essentially a mean-field description of the spatial correlation between segments i,j: in particular we choose to form the geometric mean of the convolution integrals for the following reason. It is apparent from eq 4 that even for neighboring (but not adjacent: $1 < |i - j| \ll N$) segments i,j, very long correlations ($|i - k|,|k - j| \gg |i - j|$) will be involved, corresponding to contributions from regions of the sequence remote from the pair under consideration. Now, although all component convolutions are truncated by the range of the H-function, the *product* of the convolutions most effectively suppresses the long-range contributions to $Z(ij|N)$. As we have emphasized, the IC technique is an approximation, and whilst the interaction function is explicitly included, the reduction from an $(N - 2)$-fold integral to an $(N - 2)$-fold product of integrals inevitably results in a loss of fidelity in the expression of self-interaction within the system. It is primarily this feature of the approximation which restricts its application to systems of small to intermediate molecular weight. Nevertheless, as we have seen previously, the technique is capable of successfully describing many of the configurational properties of such systems which have been subsequently confirmed on the basis of Monte Carlo simulation.

As it stands, eq 4 cannot be solved iteratively since the geometric mean Π' explicitly excludes $k = i,j$. However, by substituting eq 4 into itself we obtain

$$Z_{ij}(12|N) = H_{ij}(12)\Pi' \int H_{ik}(13)\Pi' \int Z_{il}(14|N)Z_{lk}(43|N)\ \mathrm{d}4\ H_{kj}(32) \times \Pi' \int Z_{km}(35|N)Z_{mj}(52|N)\ \mathrm{d}5\ \mathrm{d}3 \quad (5)$$

Clearly, any heterogeneous sequence of pairwise-interacting segments may be specified, while chain connectivity is preserved by setting

$$Z(i,i \pm 1|N) = \delta(r_{i,j\pm1} - \sigma_{i,j\pm1})$$

for all internal segments. This is not essential, and a harmonic or indeed any other form of interaction between adjacent segments could easily be introduced, as may fixed or harmonic bond angles between segments $i,i \pm 2$.

Evaluation of the geometric mean in (5) presupposes a knowledge of all $Z(il|N)$, $Z(lk|N)$, etc. within the sequence. In this iterative approach, however, initial guesses for the Z-functions permit a first cycle of estimates for the complete set of distributions to be formed, representing the basis for a second iterated estimate and so on until the desired degree of convergence is achieved. In practice the H-functions provide reasonable first estimates of the Z-functions, and fast Fourier transform techniques permit the rapid evaluation of the basic integral eq 5.

In the present problem we consider a perfectly flexible "pearl necklace" sequence of N identical hard-sphere segments of diameter $\sigma_i = 1$, terminated by a zeroth hard-sphere segment of diameter $\sigma_0 = 64$ which is taken to represent the effect of a rigid planar boundary. Earlier studies[5] suggest that asymptotic properties appropriate to $\sigma_0 = \infty$ are rapidly attained with increasing σ_0, and in fact

$\sigma_0 = 64$ appears quite satisfactory for chains of short to intermediate length ($N < 25$). In the absence of a solvent, direct comparisons of the IC estimates on this basis and Monte Carlo simulations at a rigid plane are in good numerical agreement.[7]

Intramolecular interference is introduced through the H-functions in eq 5 via the central pair interaction $\Phi(r_{ij})$ developed between segments i,j within the sequence. Clearly, *any* central pairwise interaction may be specified—in particular, the potential of mean force $\Psi(r_{ij}|N)$ developed in the previous section. Thus, between any pair of segments i,j we take $H(ij|\eta) = \exp(-\Psi_{\beta\beta}(r_{ij}))$, while the corresponding segment/boundary function becomes $H(0i|\eta) = \exp(-\Psi_{\alpha\beta}(r_{0i}))$ (Figure 1).

The Segment Density Distributions $\rho(z|N)$

Provided $\sigma_0 \gg \sigma_i$ and $N \ll 128\pi\sigma_i$ ensuring that the sequence is unable to "wrap around" the terminal segment, the spherical boundary may be regarded as essentially planar and a cylindrical polar coordinate frame adopted for the local chain description: Monte Carlo simulations[7] confirm this assertion. In particular we identify $r_{0i} - 32.5\sigma_i \equiv z_i$ where z_i is the normal displacement of the ith segment from the segment/boundary collision radius, and we define the segment density distribution

$$\rho(z|N)_\eta = \sum_{i=2}^{N} Z(0i|N)_\eta \qquad (6)$$

where the $Z(0i|N)_\eta$ represent the normalized boundary/segment i probability distributions at solvent packing fraction η. The most striking feature of these functions is the development of pronounced oscillations of the same period as the solvent diameter, clearly reflecting the solvent/boundary interfacial structure.

Summation over the set of $Z(0i|N)_\eta$ (eq 6) yields the segment density distribution, which at zero packing fraction corresponding to an in vacuo or solvent continuum. These results have been previously reported on the basis of both IC and Monte Carlo analyses.[6] A striking and controversial feature of these segment density distributions is the discontinuity in $\rho(z|N)_\eta$ at $z = \sigma_i$. Such a discontinuity had not been reported previously and, while essentially incapable of resolution in lattice-based analyses, is nevertheless confirmed by careful Monte Carlo simulation[7] and, furthermore, its validity has been analytically established[8] and attributed to $Z(02|N)$. The discontinuity persists over the entire range of chain lengths ($N < 20$), solvent packing fractions ($\eta = 0.00, 0.20, 0.40$), and solvent diameters ($\sigma_s = 0.0, 0.5, 1.0, 2.0$) investigated and is considered a real feature of the hard-sphere chain–plane interaction. In Figure 2 we compare the segment density distributions for $N = 15$ as a function of solvent packing fraction and solvent diameter. We observe that the solvent induces oscillations or layering in the density profile which obviously derive from the oscillations in the $Z(0i|N)_\eta$ which are evidently closely phase related. Although the discontinuity persists, it becomes somewhat difficult to distinguish from the oscillatory structure of the density profile; moreover, the location of the discontinuity is determined by the segment diameter, confirming its attribution to the chain–plane interaction, the period and amplitude of the quasi-layered structure at the boundary are established by the solvent particle diameter relative to that of the segment and packing fraction, respectively. Such interfacial structure should be experimentally discernible, although no such phenomenon has been reported in the literature. The thermodynamic consequences of a structured interface have been considered extensively for simple

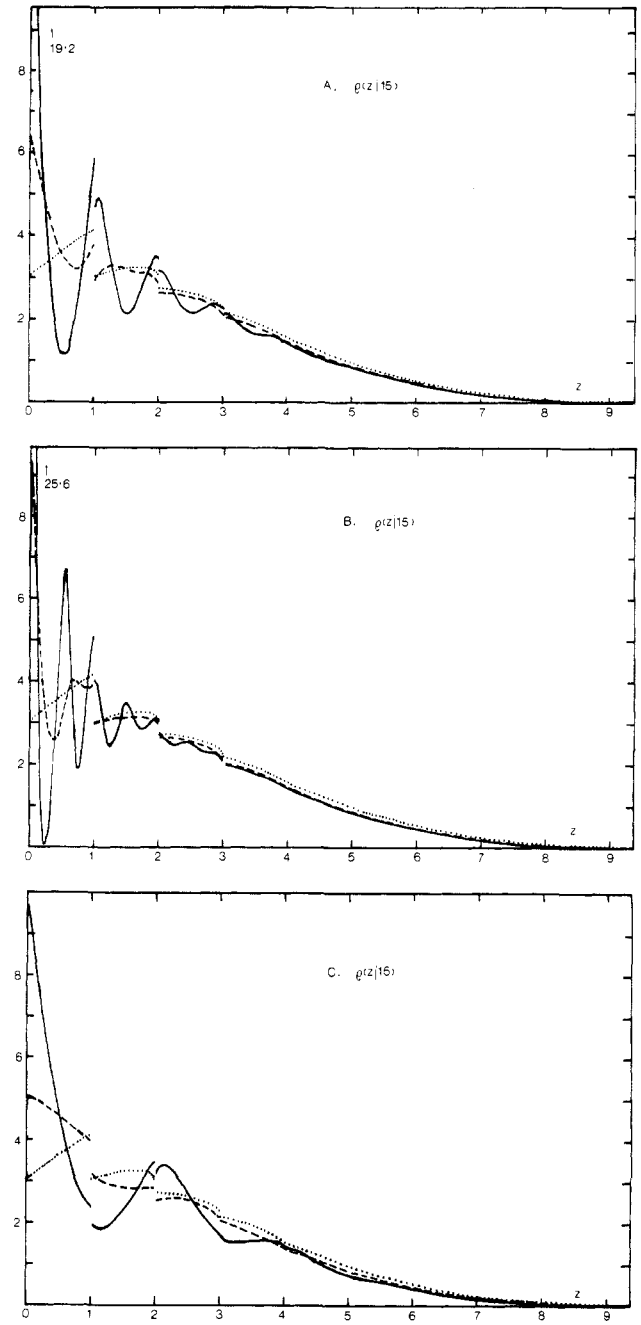

Figure 2. Segment density distribution $\rho(z|15)_\eta$ normal to the rigid boundary at various solvent compositions (η,σ_s); segment diameter is unity throughout. Solvent diameter: (A) $\sigma_s = 1.0$; (B) $\sigma_s = 0.5$; (C) $\sigma_s = 2.0$. Packing fraction: (···) $\eta = 0.0$; (- - -) $\eta = 0.2$; (—) $\eta = 0.4$.

fluid systems,[10] however, we shall not consider this aspect further here. Of particular interest is the boundary contact value of the segment density profile which develops dramatically with solvent packing fraction and inversely with solvent particle diameter. The contact value reflects the incidence of returns to the boundary by the chain, and in an earlier analysis on the basis of both the convolution approximation and Monte Carlo simulation,[7] the development of loops and trains was found to be sensitively dependent upon the contact value of the density profile. We therefore conclude that the solvent is instrumental in determining the configurational partitioning among loop, train, and tail states for sequences terminally attached to a rigid boundary. While lattice-based analyses of the development of loop, train, and tail structure have been reported, clearly those aspects related to the detailed

structural features of the solvent cannot be resolved in such caricatures.

But for the existence of the discontinuity, which is a geometric consequence of the nature of the chain–plane interaction, the density profile at zero packing fraction is essentially determined by two competing contributions to the free energy of the system: chain connectivity, tending to restrict the spatial extent of the terminally attached sequence, and an entropic component arising from configurational attrition of the chain in the vicinity of the boundary, which tends to delocalize the sequence. This entropic depletion of the segment density distribution in the immediate vicinity of the boundary is clearly apparent at zero packing fraction in Figure 2. The contribution arising from chain connectivity remains unmodified by solvent packing fraction or solvent diameter, of course; the entropic contribution to the free energy of the chain at the boundary is somewhat more subtle, however, depending whether a lower net free energy of the system (chain + solvent) is achieved by replacing solvent particles by chain segments. Clearly this will be a function of both solvent density and diameter.

Consider first of all a solvent whose particles are the same diameter as the chain segments (Figure 2A): it is evident that the mean entropy per unit area of boundary is lower for chain segments than for solvent particles due to the sequential constraints imposed upon the former. Clearly, configurational attrition per unit area due to the introduction of a boundary is minimized by replacing solvent particles by chain segments, with an associated enhancement of the segment density profile at the boundary, and this is apparent at even the lowest packing fractions investigated (Figure 2A). However, as we observed above, this situation reverses in the total absence of solvent with a depletion of segment density at the boundary (Figure 2A). With decreasing solvent diameter, replacement of solvent by segment particles at the boundary becomes progressively more appropriate if a minimization of configurational attrition, and hence excess free energy per unit area, is to be achieved. Accordingly we anticipate an increase in the boundary contact value of the segment density profile with increasing solvent density and, more particularly, with decreasing solvent diameter: both these features are confirmed in Figure 2.

As we observed above, the boundary contact value of the segment density profile is intimately related to the partitioning of chain configurations among loop, train, and tail states, and although no studies in the presence of a solvent have been reported in the literature, we anticipate on the basis of earlier MC and convolution analyses at zero packing fraction[7] that with increasing solvent packing fraction and decreasing solvent diameter there should be a progressive depopulation of tail states in favor of loop and train configurations, involving, as they do, one or more returns to the boundary.

The Mean Thickness of the Adsorbed Layer

The mean thickness of the adsorbed polymer layer is given by

$$\langle z_N \rangle_\eta = \int_0^\infty \rho(z|N)_\eta z \, dz \qquad (7)$$

and is shown as a function of chain length versus solvent packing fraction and diameter in Figure 3. Also shown for the purposes of comparison are the corresponding Monte Carlo results at zero packing fraction: we observe that the IC technique provides a good quantitative description of such systems, and that we may extend the analysis to higher solvent packing fractions with confidence.

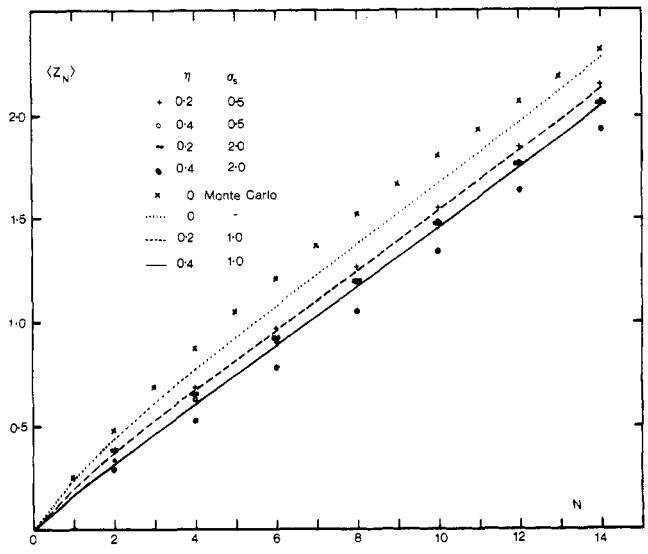

Figure 3. Mean thickness of the adsorbed layer $\langle z_N \rangle_\eta$ as a function of chain length N, solvent packing fraction η, and diameter σ_s.

It is immediately apparent from Figure 3 that the role of the solvent is to effect a reduction in the mean thickness of the adsorbed polymer, the degree of condensation at the boundary increasing with both packing fraction and solvent diameter. For example, at $N = 15$ and $\eta = 0.4$, $\langle z_N \rangle_\eta$ is reduced by about 20% by the introduction of solvent $\sigma_s = 0.5$ and by 25% for solvent $\sigma_s = 2.0$. From eq 7 we see that $\langle z_N \rangle_\eta$ is particularly sensitive to the long-range form of $\rho(z|N)_\eta$ and relatively insensitive to the structure in the vicinity of the boundary ($0 < z < 1$); indeed, $\langle z_N \rangle_\eta$ is totally independent of the boundary contact value of the segment density distribution. Moreover, we note from Figure 2 that for $z > 2.5$ segment diameters $\rho(z|N)_\eta$ is consistently below the zero solvent packing fraction curve at all solvent densities to an extent depending upon solvent packing fraction and diameter. Indeed, for large-diameter solvent particles the solvent-induced oscillations in $\rho(z|N)_\eta$ are strongly depressed below the zero packing fraction curve beyond 2.5 segment diameters, accounting at once for the behavior illustrated in Figure 3. Since it is generally accepted (e.g., ref 9 and references contained therein) that $\langle z_N \rangle_\eta$ is primarily attributable to tail configurations, we conclude that the solvent must effect some reassignment among the states from tail to loop and train configurations, certainly the latter, given the dramatic increase in boundary contact value of $\rho(z|N)$ upon introduction of the solvent.

Mean Square End-to-End Separation

The mean square end-to-end length $\langle R^2_{1N} \rangle_\eta$ is given by

$$\langle R^2_{1N} \rangle_\eta = 4\pi \int_0^\infty Z(1N|N)_\eta R_{1N}^4 \, dR_{1N} \qquad (8)$$

and was determined as a function of solvent packing fraction and diameter. Previous IC determinations at zero packing fraction appear to be in good numerical agreement with MC analyses,[7] as do earlier convolution estimates of the equation of state in dense solvents.[2,3]

Solvent-induced oscillations depress the long-range amplitude of $Z(1N|N)_\eta$ below its zero packing fraction counterpart (cf. Figure 2) to which the estimate of $\langle R_{1N}^2 \rangle_\eta$ is particularly sensitive (eq 8). Consequently there is a systematic reduction in $\langle R_{1N}^2 \rangle_\eta$ with increasing solvent

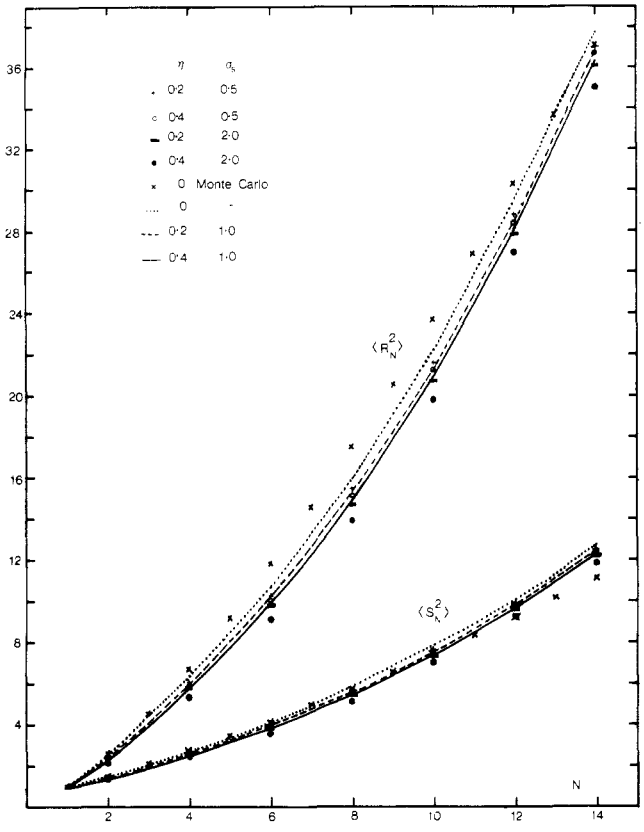

Figure 4. Effect of solvent composition (η,σ_s) upon the mean square end-to-end separation $\langle R_{1N}^2 \rangle$ and mean square radius of gyration $\langle S_N^2 \rangle_\eta$ for a terminally attached hard-sphere sequence.

packing fraction and diameter (Figure 4), much as for the thickness of the adsorbate $\langle z_N \rangle$.

The Mean Square Radius of Gyration

The mean square radius of gyration is defined as

$$\langle S_N^2 \rangle_\eta = \frac{2}{N(N-1)} \sum_{i=1}^{N-1} \sum_{j=i+1}^{N} \langle R_{ij}^2 \rangle_\eta \qquad (9)$$

and has been previously determined for terminally attached chains at zero solvent packing fraction when it was found to be in good quantitative agreement with Monte Carlo estimates.[7] $\langle S_N^2 \rangle_\eta$ is a particularly sensitive test of the IC technique, involving as it does the second moment of the complete set of internal distributions $Z(ij|N)_\eta$. The long-range form of each of these distributions is reduced in amplitude with increasing solvent packing fraction and diameter, and we anticipate similar behavior as for $\langle R_{1N}^2 \rangle_\eta$, which is confirmed in Figure 4 for the range of σ_s and η investigated.

Discussion

We have presented an analysis of the role of solvent composition in determining the structure and properties of hard-sphere sequences terminally attached to a rigid boundary. Certainly the model is artificial in the sense that perfectly flexible hard-sphere sequences are considered in a hard-sphere solvent—nevertheless, many of the configurational features of the system as they pertain to polymer adsorption are determined by excluded volume processes operating in the vicinity of the boundary, and to that extent such a simplified model is justified. Moreover, we believe such a model reflects qualitative behavior valid beyond the particular model considered here. These caricatures appear to be essential precursors in the theoretical discussion of more realistic systems, at least if the development of a statistical mechanical description is to achieve the generally satisfactory level previously attained in the theory of the liquid state.

In no sense, then, are we purporting to model any specific system, but rather to isolate those features of essentially geometric origin which appear to determine the principal features of polymer adsorption. The incorporation of more realistic interactions presents no problems in principle, although the modeling of a specific system might yet be somewhat premature. Nevertheless, experience with more realistic systems on the basis of the IC approximation does suggest that the conformational averages are modified with the introduction of attractive forces. However, until calculations for specific systems are envisaged, the introduction of more exotic interactions does not seem appropriate.

From the point of polymer adsorption, it appears that the geometric consequence of the introduction of a hard-sphere solvent is to dramatically increase the boundary contact value of the segment density profile with respect to the complete absence of solvent. We have accounted for this in terms of a minimization of the free energy of the chain + solvent system. The consequences of this enhancement of the contact value is the increased development of loop and train configurations at the boundary, and this is the subject of a forthcoming publication.[12] In addition, the segment density profile acquires a *layered* structure which clearly reflects the packing of solvent particles at the rigid boundary—the period of the layering being that of the solvent diameter, while the amplitude increases with solvent packing fraction.

The introduction of solvent appears to reduce the thickness of the adsorbed layer $\langle z_N \rangle$ to an extent depending both upon solvent diameter and packing fraction, which again reflects the transition from tail to loop and train configurations.[12] Indeed, in the absence of a solvent, tail configurations accounted almost entirely for the constitution of the adsorbed layer.[6] Certainly the introduction of an attractive chain–plane interaction substantially modifies the constitution of the adsorbate in terms of its loop, train, and tail components[9] and we anticipate that this would be further complicated by the introduction of a realistic solvent. For present purposes, however, restriction to a simple excluded-volume model is appropriate, particularly if comparison is to be made at some stage with computer simulation data.

Finally, we note that the present results relating to the development of $\langle R_{1N}^2 \rangle_\eta$ and $\langle S_N^2 \rangle_\eta$ with solvent composition are in qualitative agreement with the recent studies of Bishop et al.[13] Direct comparison with their investigations is not possible however, since they are concerned with scaling relations in isolated multichain systems. Nevertheless, a pronounced reduction in both $\langle R_{1N}^2 \rangle_\eta$ and $\langle S_N^2 \rangle_\eta$ with increasing chain packing fraction is observed, and this incidentally also concurs with a much earlier convolution description for isolated sequences.[2]

Acknowledgment. I thank Ruby Turner for performing the numerical computations and ARGS for financial support.

References and Notes

(1) Bellemans, A.; de Vos, E. *J. Polym. Sci., Polym. Symp.* **1973**, *42*, 1195.
(2) Croxton, C. A. *J. Phys. A.: Math. Gen.* **1979**, *12*, 2497.
(3) Dickman, R.; Hall, C. K., to be published.
(4) Croxton, C. A. *J. Phys. A: Math. Gen.* **1984**, *17*, 2129.
(5) Croxton, C. A. *Faraday Symp. Chem. Soc.* **1981**, *16*, 91.
(6) Flocculation and stabilization of polymers (Croxton, C. A. *J. Phys. A: Math. Gen.* **1983**, *16*, 4343), ring polymers (*Ibid.*

1985, *18*, 995), loops, trains, and tails (*Ibid.* 1986, *19*, 2353), and stars (Croxton, C. A. submitted for publication in *Macromolecules*).
(7) Croxton, C. A. *J. Phys. A: Math. Gen.* 1986, *19*, 987.
(8) Croxton, C. A. *Phys. Lett. A* 1985, *111*, 453.
(9) Croxton, C. A. In *Fluid Interfacial Phenomena*; Croxton, C. A., Ed.; Wiley: Chichester and New York, 1986; Chapter 7, p 343 ff.
(10) Croxton, C. A. *Statistical Mechanics of the Liquid Surface*; Wiley: Chichester and New York, 1980.
(11) Pratt, L. R.; Chandler, D. *J. Chem. Phys.* 1977, *67*, 3683.
(12) Croxton, C. A. to be published in *Macromolecules*.
(13) Bishop, M.; Kalos, M. H.; Sokal, A. D. *J. Chem. Phys.* 1983, *79*, 3496.

Molecular Weights and Solution Properties of a Series of Side-Chain Liquid Crystalline Polymers with Ethylene Oxide Spacers

R. Duran*† and C. Strazielle

Institut Charles Sadron (CRM-EAHP), Strasbourg, Cedex 67083, France.
Received December 3, 1986

ABSTRACT: A homologous series of methacrylate side-chain liquid crystalline (LC) homopolymers and copolymers was studied in solution by several techniques. The molecular weight distributions and some hydrodynamic and thermodynamic parameters were calculated. A decrease in the dn/dc values of the copolymers compared to those of their corresponding homopolymers was attributed to a higher density in solution of the homopolymers presumably caused by biphenyl–biphenyl interaction. A large discrepancy was found between the molecular weights found by classical size exclusion chromatography and those found by direct methods. Also an odd–even effect as a function of spacer length was seen in the exponent of the viscosity law and the Flory χ value.

Introduction

Though much research has been done on side-chain liquid crystalline (LC) polymers in the solid state,[1,2] to date relatively little attention has been paid to the properties of these polymers in solution.[3,4] Knowledge of solution properties, however, can be helpful in several ways. First and most obviously, solution properties must be known to be sure of correct molecular weight determination by all but chemical methods. Often molecular weights are claimed by size exclusion chromatography (SEC) or viscosometric methods which have been calibrated with polymers having entirely different properties than LC polymers. Second, it is thought that knowledge of the hydrodynamic properties of side-chain LC polymers in solution can give valuable insights into their solid-state behavior. Third, studies of these types of polymers are inherently interesting insofar as they can lead to a better understanding of the solution state.

It was therefore interesting to compare the results obtained for a series of side-chain LC polymers studied by several techniques: SEC, light scattering coupled SEC (LS–SEC) and classical light scattering (LS) in solution. These techniques can also give complementary thermodynamic and hydrodynamic parameters which permit further understanding of these LC polymers in solution.

As part of a collaborative effort, we are interested in LC polymers with ethylene oxide spacers; the polymer synthesis, liquid crystalline properties, and structural characterization are reported elsewhere.[5–7] The polymers studied here consisted of two homologous series. The first was a series of homopolymers with a methacrylate backbone to which was attached an oligo(ethylene oxide) spacer with a methoxybiphenyl mesogenic group as shown below. The spacer length varied from zero, i.e., the methoxybiphenyl attached directly to the backbone, to four ethylene oxide units, i.e. a tetrakis(ethylene oxide) spacer. In the text, these polymers are referred to by the abbreviation PM- with a number indicating the length of the spacer. For example, PM-2 indicates the methacrylate homopolymer with a bis(ethylene oxide) spacer. A series of four random methacrylate copolymers was also studied. These copolymers contained two different length spacers in a 50% ratio. They are abbreviated by PM- with two numbers separated by a comma indicating the respective spacer lengths; for example, PM-2,3 indicates the methacrylate copolymer of monomers with a bis(ethylene oxide) and a tris(ethylene oxide) spacer, respectively.

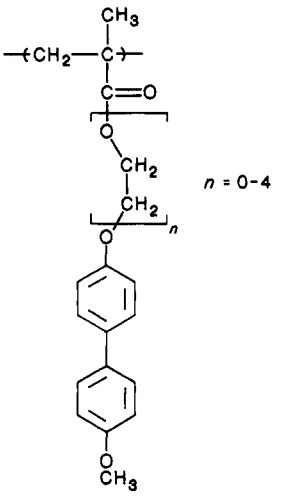

Experimental Section

(A) Samples. The series of methacrylate homopolymers and copolymers used in this study were synthesized in the laboratory of Ph. Gramain at the ICS, Strasbourg. Their synthesis and characterization has been described elsewhere.[6] THF and $CHCl_3$ used for the solutions were dried and distilled twice before use.

(B) Methods. (i) Light Scattering (LS). Weight-average molecular weights, M_w, were determined in THF or $CHCl_3$ solutions by a Fica 50 instrument. Measurements were made with

†Current address: Max Planck Institut fur Polymerforschung, D6500, Mainz, FRG.

0024-9297/87/2220-2853$01.50/0